OPEN

Curcumin-mediated Photodynamic Therapy Inhibits the Phenotypic Transformation, Migration, and Foaming of Oxidized Low-density Lipoprotein-treated Vascular Smooth Muscle Cells by Promoting Autophagy

Gailan Wang, BS, Ying Zhu, MD,* Kaiting Li, MM,* Bo Liao, BS,* Fang Wang, BS,* Lan Shao, MM,* Liyi Huang, MM,†‡ and Dingqun Bai, MD**

Abstract: Vascular smooth muscle cells (VSMCs) are becoming a hot spot and target of atherosclerosis research. This study aimed to observe the specific effects of curcumin (CUR)-mediated photodynamic therapy (CUR-PDT) on oxidized low-density lipoprotein (ox-LDL)-treated VSMCs and confirm whether these effects are mediated by autophagy. In this study, the mouse aortic smooth muscle cell line and A7r5 cell lines were used for parallel experiments. VSMC viability was evaluated by Cell Counting Kit-8 assay. VSMCs were treated with ox-LDL to establish a model of atherosclerosis in vitro. The autophagy level and the expression of proteins related to phenotypic transformation were detected by western blotting. The migration ability of the cells was detected by using transwell assay. The presence of intracellular lipid droplets was detected by Oil Red O staining. The results showed that VSMCs transformed from the contraction phenotype to the synthetic phenotype when stimulated by ox-LDL, during which autophagy was inhibited. However, CUR-PDT treatment significantly promoted the level of autophagy and inhibited the process of phenotypic transformation induced by ox-LDL. In addition, ox-LDL significantly promoted VSMC migration and increased the number of lipid droplets, whereas CUR-PDT treatment significantly reduced the ox-LDL-induced increase in the migration ability of, and lipid droplet numbers in, VSMCs. When the VSMCs were pretreated with the autophagy inhibitor 3-methyladenine for 24 hours, the effects of CUR-PDT were reversed. Therefore, our study indicated that CUR-PDT can inhibit the phenotypic transformation, migration, and foaming of ox-LDL–treated VSMCs by inducing autophagy.

Key Words: atherosclerosis, vascular smooth muscle cells, photodynamic therapy, curcumin, autophagy

(*J Cardiovasc Pharmacol*™ 2021;78:308–318)

INTRODUCTION

Atherosclerosis (AS) is a disease mainly based on lipid metabolism disorder and typically manifests as thickening of the arterial wall and narrowing of the vascular lumen.[1] At present, AS is the primary cause of cardiovascular and cerebrovascular diseases.[1] Therefore, new therapeutic targets and strategies for AS have been widely explored. Vascular smooth muscle cells (VSMCs) are located in the vascular media membrane.[2] In the normal functional state, VSMCs show a contraction phenotype with a high degree of differentiation and poor or no proliferation and migration ability, and their main functions are to maintain vascular elasticity, vasoconstriction, and blood pressure regulation.[2] It has been reported that when blood vessels are damaged or stimulated by oxidized low-density lipoprotein (ox-LDL), the normal VSMC contraction phenotype converts to an abnormal synthetic phenotype with a low degree of differentiation, leading to VSMC migration into the intima and the phagocytosis of cholesterol, which results in lipid accumulation and the formation of foam cells, eventually reducing plaque stability and further accelerating AS development.[3–6] Foam cells have always been a key starting point for the prevention and treatment of AS. Relevant studies showed that only 30% of foam cells in middle and late atherosclerotic plaques are derived from macrophages, whereas more than 40% are derived from VSMCs.[7,8] Therefore, inhibiting the transformation of VSMCs to the synthetic phenotype and foam-like changes plays a positive protective role in the prevention and treatment of AS.

Received for publication January 6, 2021; accepted May 2, 2021.

From the *Department of Rehabilitation Medicine, the First Affiliated Hospital of Chongqing Medical University, Chongqing, China; †Department of Rehabilitation Medicine Center, West China Hospital, Sichuan University, Chengdu, China; and ‡Key Laboratory of Rehabilitation Medicine in Sichuan Province, Chengdu, China.

Supported by grants from the National Natural Science Foundation of China (grant number: 8187090832).

The authors report no conflicts of interest.

Supplemental digital content is available for this article. Direct URL citations appear in the printed text and are provided in the HTML and PDF versions of this article on the journal's Web site (www.jcvp.org).

Conceptualization: Y. Zhu and D. Bai; Data curation: G. Wang, Y. Zhu and D. Bai; Formal analysis: G. Wang, Y. Zhu, and K. Li; Funding acquisition: D. Bai; Methodology: G. Wang, B. Liao, F. Wang, L. Shao, and L. Huang; Project administration: D. Bai; Resources: Y. Zhu, L. Huang, and D. Bai; Software: G. Wang, B. Liao, and L. Shao; Validation: G. Wang and K. Li; Visualization: G. Wang and F. Wang; Writing-original draft: G. Wang; Writing-review and editing: G. Wang, Y. Zhu, K. Li, and D. Bai.

Correspondence: Dingqun Bai, MD, Department of Rehabilitation Medicine, the First Affiliated Hospital of Chongqing Medical University, Chongqing 400010, China (e-mail: baidingqun2014@163.com).

Curcumin (CUR) is a type of polyphenol compound extracted from the rhizome of *Curcuma longa,* and studies have shown that curcumin has antitumor, anti-inflammatory, antioxidant, anti-AS, anti-lipid, other pharmacological activities, and photosensitive properties.[9–13] Photodynamic therapy (PDT) is a novel approach to the treatment of specific diseases with photosensitizers and laser activation.[14] Irradiation of the target tissue with a specific wavelength can activate photosensitive drugs selectively gathered in the target tissue and induce photochemical reactions to promote autophagy, apoptosis, and necrosis of the diseased tissue cells.[14–16] Studies have shown that atherosclerotic plaques have a characteristic effect on the absorption and retention of curcumin.[17] Therefore, the synergy between curcumin and photodynamic therapy may serve as a novel idea strategy for the prevention and treatment of AS.

Autophagy is a process in which cytoplasmic proteins or organelles are engulfed into vesicles and fused with lysosomes to form autolysosomes and degrade their contents, thus achieving the metabolic requirements of the cell and renewal of some organelles.[18] Autophagy is involved in many physiological and pathological processes, and whether its role is positive or negative is not completely clear.[4,19] VSMC autophagy plays an important role in the development of AS.[20,21] Recent studies showed that activation of autophagy could inhibit intimal hyperplasia and the formation of AS plaques mainly by inhibiting the transformation of VSMCs from the contraction phenotype to the synthetic phenotype and weakening their proliferation and migration capacity.[22] In addition, studies have confirmed that autophagy can inhibit the formation of VSMC-derived foam cells by mediating the lysosomal degradation of lipid droplets in VSMCs.[23] Therefore, induction of autophagy in VSMCs is expected to provide new avenues for the treatment of AS.

Studies related to AS have confirmed that PDT can promote the excretion of cholesterol by inducing autophagy of macrophages and reducing the transformation of macrophages into foam cells.[24] However, the regulation of autophagy in VSMCs by CUR-PDT and the specific role of CUR-PDT in inhibiting AS progression are still unclear. To address this issue, herein, we investigated whether CUR-PDT attenuated phenotypic transformation and foam-like changes by autophagy in ox-LDL–treated VSMCs. It is expected to provide new theoretical support for the treatment of AS.

MATERIALS AND METHODS

Materials

Dulbecco's modified Eagle's medium (DMEM) and fetal bovine serum (FBS) were purchased from Gibco (Grand Island, NY). Cell Counting Kit-8 (CCK-8) was purchased from Dojindo Molecular Technologies (Kumamoto, Japan). Ox-LDL was purchased from Yiyuan Biotechnology (Guangzhou, China). Curcumin and Oil Red O were purchased from Sigma-Aldrich (St Louis, MO). Curcumin was dissolved in dimethyl sulfoxide (Sigma-Aldrich, St Louis, MO) and stored at −20°C, and Oil Red O was dissolved in isopropanol and stored at 4°C. Primary antibodies against LC3B, Beclin-1, p62, and the internal reference antibody (anti-β-actin) were purchased from Cell Signaling Technology (CST, Danvers, MA). The primary antibodies anti-α- smooth muscle actin (SMA), anti-SM22-α, and anti-osteopontin (OPN) were purchased from Abcam (Cambridge, United Kingdom). Goat anti-rabbit secondary antibody was purchased from CST (Danvers, MA). The autophagy inhibitor 3-methyladenine (3-MA) was purchased from MedChemExpress (MCE, NJ). Four percent paraformaldehyde was purchased from Boster Biological Technology (Wuhan, China). Hematoxylin was purchased from Solarbio (Beijing, China). The 0.1% crystal violet dye solution, protein lysis buffer RIPA and phenylmethanesulfonyl fluoride, bicinchoninic acid kit, and sodium dodecyl sulfate-polyacrylamide gel electrophoresis Gel Quick Preparation Kit were purchased from Beyotime (Shanghai, China).

Cell Culture

The mouse aortic smooth muscle cell line (MOVAS) and rat thoracic aorta cell line (A7r5) were cultured in DMEM containing 10% FBS and 1% penicillin-streptomycin and incubated in a humidified incubator containing 5% CO_2 at 37°C. The cells were digested with 0.05% trypsin and collected. The cells were centrifuged at 1000 rpm for 3 minutes. Then, the cells were transferred to several new culture bottles for further culture according to the number of cells. Untreated cells were used as controls.

CUR-PDT Processing Steps

Curcumin was dissolved in dimethyl sulfoxide to 10 mmol/L and stored at −20°C in the dark. In this study, the working concentration of curcumin was 20 μmol/L according to the experimental results of CCK-8 assay. VSMCs were randomly divided into control, CUR, Laser, and CUR-PDT groups. After the cells attached to the wall, the culture medium of the CUR group and the CUR-PDT group was replaced with 20 μmol/L CUR, and the DMEM medium of the same volume was added to the control group and Laser group, and all groups were incubated in the dark under the above conditions. After 12 hours, the medium was removed, the cells were washed twice with phosphate-buffered saline (PBS), and fresh DMEM medium was added. The Laser and the CUR-PDT groups were subjected to corresponding light irradiation (425 nm, 40 mW/cm^2) while the other groups were kept in the dark. The cells were incubated for 6 hours and then analyzed differently. For inhibitory studies, 5 mmol/L of the autophagy inhibitor 3-MA was used for intervention before CUR-PDT.

Cell Viability Assay

CCK-8 was performed according to the manufacturer's instructions. In brief, the VSMCs were seeded into a 96-well plate, and each group was prepared with 5 duplicates. The VSMCs were cultured until they had adhered to the wall in an incubator containing 5% CO_2 at 37°C. After the different interventions, all groups were treated with DMEM medium containing CCK8 (DMEM: CCK-8 = 9:1), including the blank control group (DMEM only, no cells), negative control group (with DMEM, with cells), and all experimental groups (with DMEM, cells, treatment factors). The cells were

incubated in the dark for 4 hours in a 5% CO_2 incubator at 37°C, and the optical density (OD) value at a wavelength of 450 nm was measured with a microplate reader. Finally, the following formula was used to calculate the survival rates of VSMCs: survival rate = (average OD value of experimental group − average OD value of blank control group)/(average OD value of negative control group − average OD value of blank control group) ×100%. The experiment was repeated 3 times.

Determination of Intracellular Reactive Oxygen Species

The production of intracellular reactive oxygen species (ROS) was determined based on the presence of dichlorofluorescein diacetate (DCFH-DA). VSMCs were seeded into 12-well plates. After CUR-PDT treatment, the cells were incubated in the dark for 30 minutes. The cells were then washed 2 times with PBS, and DMEM medium containing 10 μmol/L DCFH-DA was added to each group and incubated in the dark for 30 minutes, followed by washing twice with PBS, and the green fluorescence intensity was observed under a fluorescence microscope.

Oil Red O Staining

VSMCs were seeded into 6-well plates. After the different treatment, the cells were fixed with 4% paraformaldehyde for 30 minutes and washed 3 times with PBS. The cells were then dyed with Oil Red O working solution (prepared and filtered with 0.5% Oil Red O: distilled water = 3:2) in the dark for 30 minutes at room temperature. Then, the staining fluid was carefully removed, followed by addition of 60% isopropyl alcohol for 3–5 seconds to eliminate nonspecific staining and washed with distilled water 3 times. Finally, the cells were redyed with hematoxylin for 1 minute and washed with distilled water 3 times to obtain the blue color again. The staining of lipid droplets in the cells was observed under an inverted microscope.

Transwell Assay

VSMCs were seeded into 6-well plates. After treatment with different intervention measures, all group cells were digested, labeled, and centrifuged. The supernatant was discarded, and the cells were resuspended in serum-free DMEM medium. Transwell chambers (Corning, NY) were placed in the 24-well plates, 800 μL of DMEM medium containing 20% FBS was added to the lower chamber, and 200 μL of serum-free DMEM medium was added to the upper chamber. Each group was seeded into the upper chamber with 6×10^4 cells and incubated in an incubator containing 5% CO_2 at 37°C. After 24 hours, the medium in the upper and lower chambers was removed and discarded, and the upper and lower chambers were washed 3 times with PBS. The chamber was fixed with 4% paraformaldehyde for 30 minutes and washed 3 times with PBS. Next, 800 μL of 0.1% crystal violet dye solution was added to each chamber and incubated at room temperature for 15 minutes. The cells were cleaned in a beaker filled with distilled water 3 times. Finally, the cells in the upper chamber were gently wiped away with a cotton swab. Each chamber was placed in an empty, dry hole under an inverted microscope to observe cell staining. It is important to note that the bottom of the chamber should not be touched during all operations.

Western Blot Analysis

After CUR-PDT treatment for approximately 6 hours, the total protein was extracted with protein lysis buffer RIPA and phenylmethanesulfonyl fluoride on the ice, centrifuged at ×12,000*g* at 4°C for 15 minutes, and the supernatant was obtained. The bicinchoninic acid kit was used to quantitatively determine the OD value of each group at 562 nm and calculate the protein concentration in each group. The proteins were prepared as the same volume and concentration, and then boiled at 100°C for 10 minutes to denature the proteins. After gel electrophoresis using 12% sodium dodecyl sulfate-polyacrylamide gel electrophoresis, the protein samples in each group (20–50 μg) were transferred onto a 0.22-μm polyvinylidene difluoride membrane. The samples were then blocked for 2 hours with 5% low-fat milk diluted with Tris-buffered saline Tween-20 (TBST, TBS solution: Tween-20 = 1000:1). After washing 3–5 times with TBST, the membrane and primary antibodies including anti-α-SMA (ab32575, 1:2500, Abcam), anti-SM22-α (ab155272, 1:1000, Abcam), anti-OPN (ab8448, 1:1000, Abcam), anti-LC3B (3868, 1:1000, CST), anti-Beclin-1 (3495, 1:1000, CST), anti-p62 (23,214, 1:1000, CST), and anti-β-actin (8457, 1:1000, CST) were incubated at 4°C overnight. After washing with TBST, the membrane was incubated with horseradish peroxidase–conjugated secondary antibody (7074, 1:2000, CST) at room temperature for 1 hour. The protein bands were then washed with TBST again and developed in a gel imager with chemiluminescence reagent (Thermo Fisher Scientific). The experiment was repeated 3 times. Finally, ImageJ software was used for statistical analysis.

Statistical Analysis

Statistical analysis was performed using GraphPad Prism software version 8.0. Data are expressed as the mean ± SD. Statistical analysis for multiple comparisons was performed by one-way analysis of variance. The differences between 2 groups were analyzed by the Student's *t*-test. $P < 0.05$ was considered as statistically significant ($^*P < 0.05$, $^{**}P < 0.01$, $^{***}P < 0.001$).

RESULTS

CUR-PDT Promoted ROS Production Under the Optimal CUR-mediated PDT Conditions in VSMCs

To choose the optimal treatment concentrations of curcumin and light dose, VSMCs were treated with the different concentrations of curcumin (0, 5, 10, 20, 40, and 80 μmol/L) for different time (12, 24, and 48 hours) and then were treated on the basis of the curcumin concentrations to determine the different illumination times (0, 30, 60, 90, 120, 150, and 180 seconds) at the power density of 40 mW/cm^2 with different light energy densities (0, 1.2, 2.4, 3.6, 4.8, 6.0,

and 7.2 J/cm^2). CCK-8 assay was then used to measure cell activity. The results showed that low concentrations of curcumin (≤20 μmol/L) had no significant effect on VSMC activity compared with the control groups, whereas a high concentration of curcumin (>20 μmol/L) significantly reduced the cell activity of VSMCs in a dose-dependent and time-dependent manner (Figs. 1A, B). Regarding the determination of light dose, the light intensity ≤4.8 J/cm^2 had no significant effect on the cell activity of MOVAS, whereas the light intensity >4.8 J/cm^2 decreased the cell

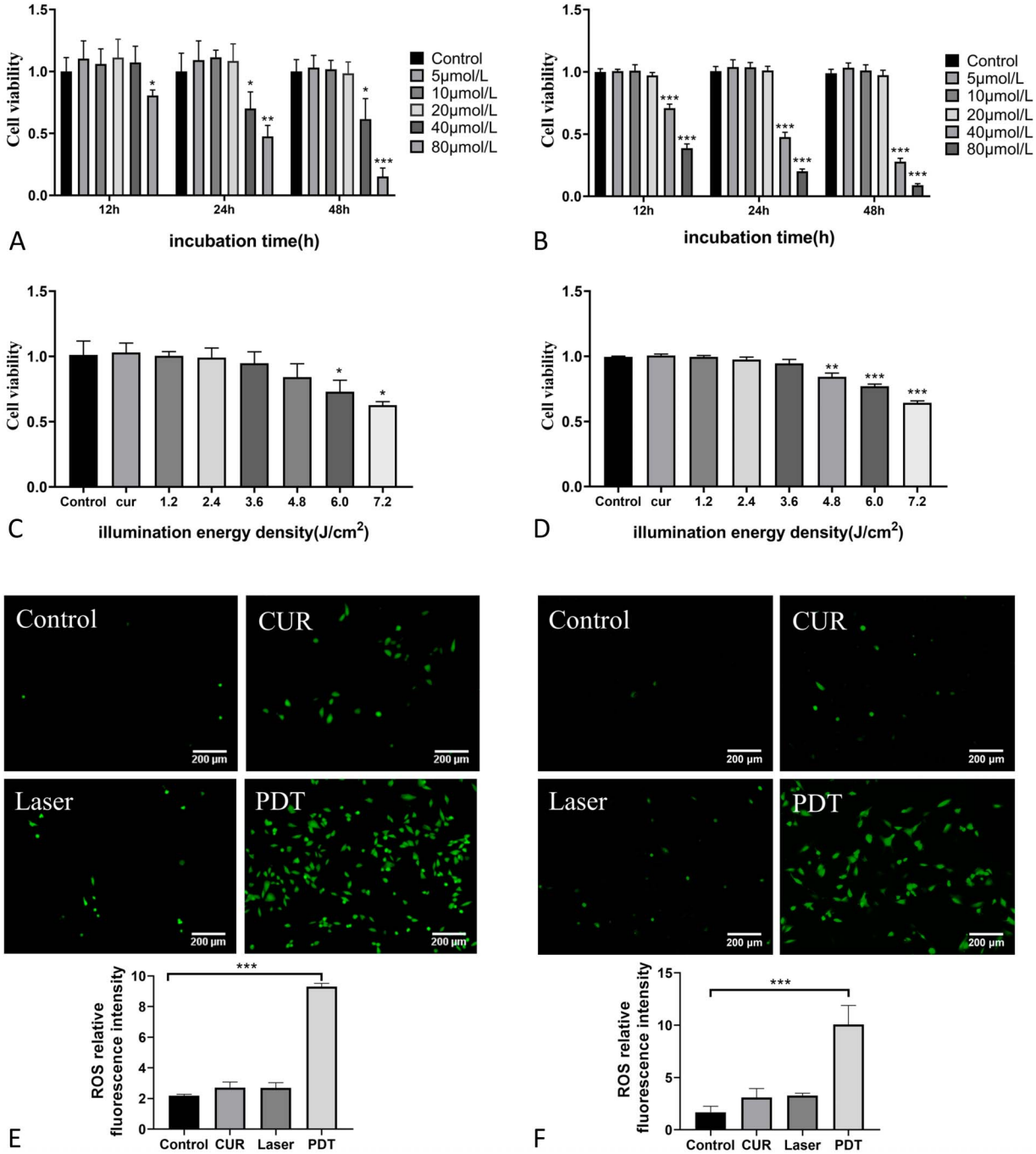

FIGURE 1. Effect of different concentrations of CUR and different energy densities on VSMCs cell activity by CCK-8 assay and detection of ROS production by DCFH-DA. A, Effect of different concentrations of CUR on MOVAS cell viability after different treatment times; (B) effect of different concentrations of CUR on A7r5 cell viability after different treatment times; (C) effects of different energy densities on MOVAS cell activity (20 μmol/L CUR); (D) effects of different energy densities on A7r5 cell activity (20 μmol/L CUR); (E) effect of CUR-PDT on ROS production in MOVAS; and (F) effect of CUR-PDT on ROS production in A7r5. n = 3 (3 independent experiments). Data are expressed as the mean ± SD. *$P < 0.0$, **$P < 0.01$, ***$P < 0.001$.

activity in an intensity dose-dependent manner (Fig. 1C). For A7r5 cells, light intensity $\leq$3.6 J/cm^2 had no significant effect on cell activity, whereas light intensity >3.6 J/cm^2 showed a dose-dependent decrease on cell activity (Fig. 1D). Therefore, 20 μmol/L CUR and 4.8 J/cm^2 light dose were selected as the optimal CUR-PDT treatment conditions for MOVAS cells, and 20 μmol/L CUR and 3.6 J/cm^2 light dose were selected as the optimal CUR-PDT treatment conditions for A7r5 cells.

In PDT, ROS are mainly produced to cause a series of effects.[25] Therefore, ROS production is the basis for PDT. According to the treatment conditions of CUR-PDT described above, VSMCs were randomly divided into 4 groups: the control group, CUR group (curcumin alone), Laser group (illumination alone), and PDT group (CUR combined illumination). Each group was given corresponding treatment respectively. Finally, ROS probe DCFH-DA was used to observe the treatment effects under a fluorescence microscope. The results showed that compared with the control group, the CUR group and the Laser group had a little fluorescence signal but without statistical difference, whereas the CUR-PDT group exhibited a significantly enhanced green fluorescence signal (Figs. 1E, F), indicating that CUR-PDT promoted ROS production in VSMCs.

CUR-PDT Inhibited Phenotypic Transformation, Migration, and Foaming of ox-LDL–treated VSMCs

To study the specific role of CUR-PDT on VSMCs in inhibiting plaque progression, ox-LDL–treated VSMCs were subjected to CUR-PDT. Western blotting was used to detect phenotypic transformation-related proteins. The results showed that the expression of VSMC contraction phenotypic markers α-SMA and SM22-α were significantly decreased in the ox-LDL group compared with that in the control group, whereas the expression of synthetic phenotypic marker OPN was significantly increased (Figs. 2A, B).The results indicated that ox-LDL could induce the transformation of VSMCs from the normal contraction phenotype to the synthetic phenotype, which would promote AS development to a large extent. After CUR-PDT treatment, the CUR and Laser groups showed no significant difference compared with the ox-LDL group. However, the contraction phenotypic proteins α-SMA and SM22-α were upregulated and the expression of the synthetic phenotypic protein OPN was downregulated in the PDT group compared with the ox-LDL group (Figs. 2A, B). This suggests that CUR-PDT can inhibit phenotypic transformation in VSMCs to slow the progression of AS. In this study, transwell assay was used to detect the migration ability of VSMCs. The results showed that ox-LDL significantly promoted VSMC migration compared with the control group. After CUR-PDT treatment, there was no significant difference in the CUR and Laser alone groups, whereas migration of VSMCs was significantly reduced in the PDT group compared with the ox-LDL group (Figs. 2C, D). These results indicated that CUR-PDT could inhibit the migration of ox-LDL–treated VSMCs. Oil Red O was used to detect lipid droplet in VSMCs. The results showed that ox-LDL significantly promoted lipid droplets accumulation in VSMCs compared with the control group. After CUR-PDT treatment, the lipid droplet accumulation degree was significantly reduced when compared with the ox-LDL group, CUR alone group, and Laser alone group (Figs. 2E, F). This indicates that CUR-PDT could inhibit lipid droplets accumulation in ox-LDL–treated VSMCs. Overall, these results show that CUR-PDT can inhibit phenotypic transformation, migration, and foaming of VSMCs to attenuate AS development and thus may be useful for the treatment of AS.

CUR-PDT Induced Autophagy in VSMCs

To confirm whether CUR-PDT can induce autophagy in VSMCs, we detected the autophagy-related markers Beclin-1, LC3B-II, and p62. The results showed that PDT remarkably increased the expression of Beclin-1 and LC3B-II and decreased that of p62 compared with the control group (Figs. 3A, B). Furthermore, CUR-PDT was used to treat ox-LDL–treated VSMCs. We found that ox-LDL significantly reduced the expression of Beclin-1 and LC3B-II and enhanced the accumulation of p62 (Figs. 3C, D). These data demonstrated that ox-LDL could hamper autophagy in VSMCs. However, CUR-PDT upregulated the expression of LC3B-II and Beclin-1 and downregulated the expression of p62 compared with the ox-LDL group (Figs. 3C, D). These results suggest that CUR-PDT can facilitate the autophagy level in VSMCs stimulated by ox-LDL, implying that CUR-PDT may regulate its phenotype and foaming by promoting VSMC autophagy.

Inhibition of Autophagy Negated the Effects of CUR-PDT on ox-LDL–treated VSMCs

To investigate whether inhibition of autophagy could attenuated the effect of CUR-PDT on ox-LDL–treated VSMCs, we pretreated VSMCs with the autophagy inhibitor 3-MA. Western blotting was used to detect the expression of autophagy-related proteins Beclin-1, p62, LC3B-II, and phenotypic transformation-related proteins α-SMA, SM22-α, and OPN. The results showed that the presence of 3-MA significantly inhibited the level of autophagy in VSMCs and negated the effect of CUR-PDT on VSMC phenotype transformation (Figs. 4A, B). Evaluation of the migration ability and lipid droplet accumulation degree were detected, respectively, by the transwell assay and Oil Red O. The results showed that 3-MA reversed the inhibition effects of CUR-PDT on VSMC migration and lipid droplet accumulation (Figs. 5A–D). Therefore, we confirmed that CUR-PDT inhibited the phenotypic transformation, migration ability, and lipid droplet accumulation degree of ox-LDL–treated VSMCs by inducing autophagy.

DISCUSSION

In recent years, PDT has been applied to the treatment of AS, but related studies have been mainly focused on macrophages.[24] VSMCs are an important component of the vascular wall and are involved in the development of AS.[2] Therefore, to elucidate the regulation of PDT on autophagy and its specific role in VSMCs, we established an AS model in vitro for the study. In this study, we demonstrate for the

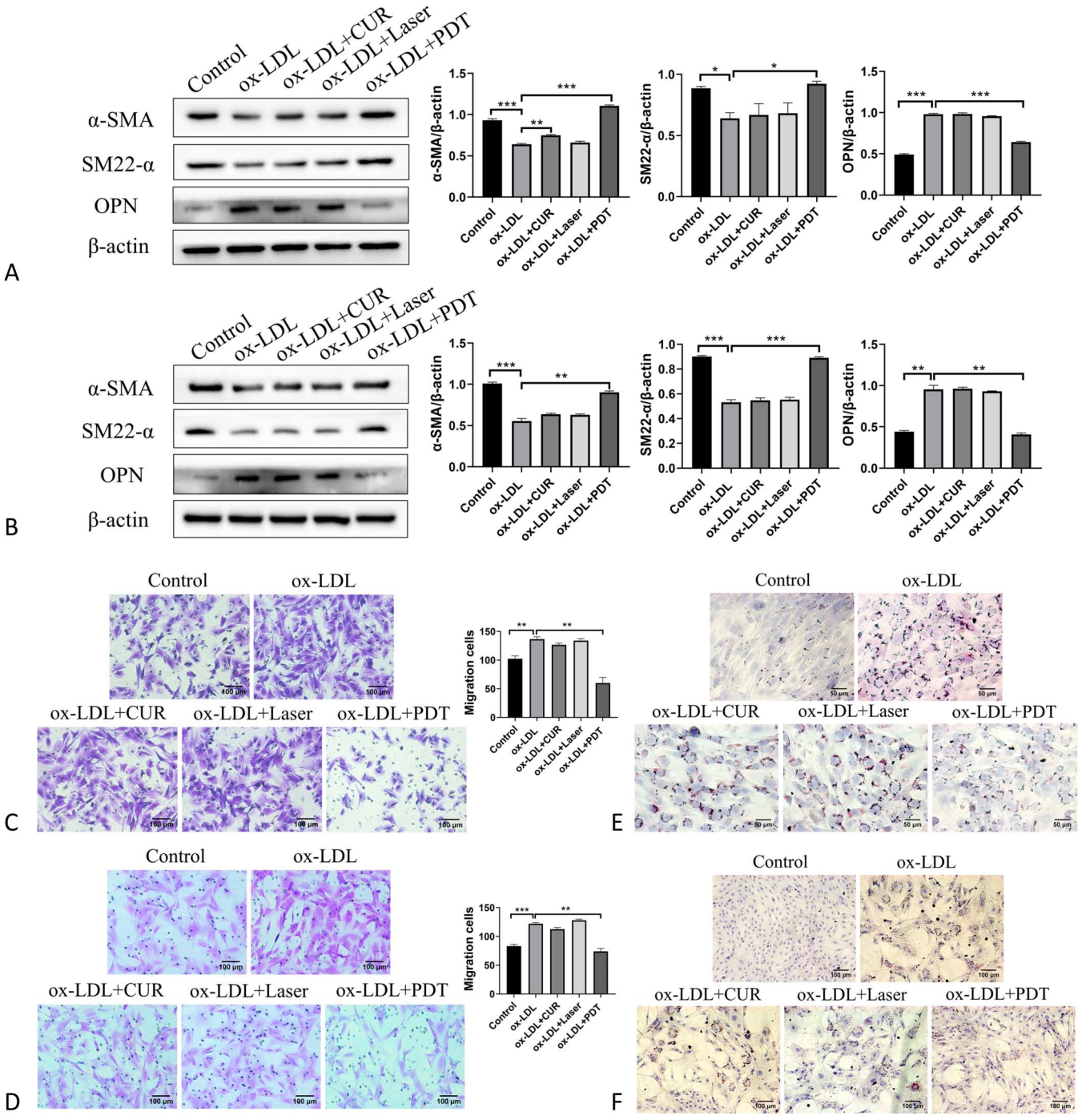

FIGURE 2. CUR-PDT inhibited the phenotypic transformation, migration, and foaming of ox-LDL–treated VSMCs. The expression of proteins related to phenotype transformation (α-SMA, SM22-α, and OPN) was detected by western blotting after different treatments for 6 hours. The migration of VSMCs was detected by transwell assay. The accumulation of lipid droplets in VSMCs was measured by Oil Red O staining after CUR-PDT. A, Effect of CUR-PDT on the expression of proteins related to phenotype transformation in ox-LDL–treated MOVAS cells; (B) effect of CUR-PDT on the expression of proteins related to phenotype transformation in ox-LDL–treated A7r5 cells; (C) effect of CUR-PDT on migration of ox-LDL–treated MOVAS cells; (D) effect of CUR-PDT on migration of ox-LDL–treated A7r5 cells; (E) effect of CUR-PDT on accumulation of lipid droplets in ox-LDL–treated MOVAS cells; and (F) effect of CUR-PDT on accumulation of lipid droplets in ox-LDL–treated A7r5 cells. n = 3 (3 independent experiments). Data are expressed as the mean ± SD. *$P < 0.05$, **$P < 0.01$, ***$P < 0.001$.

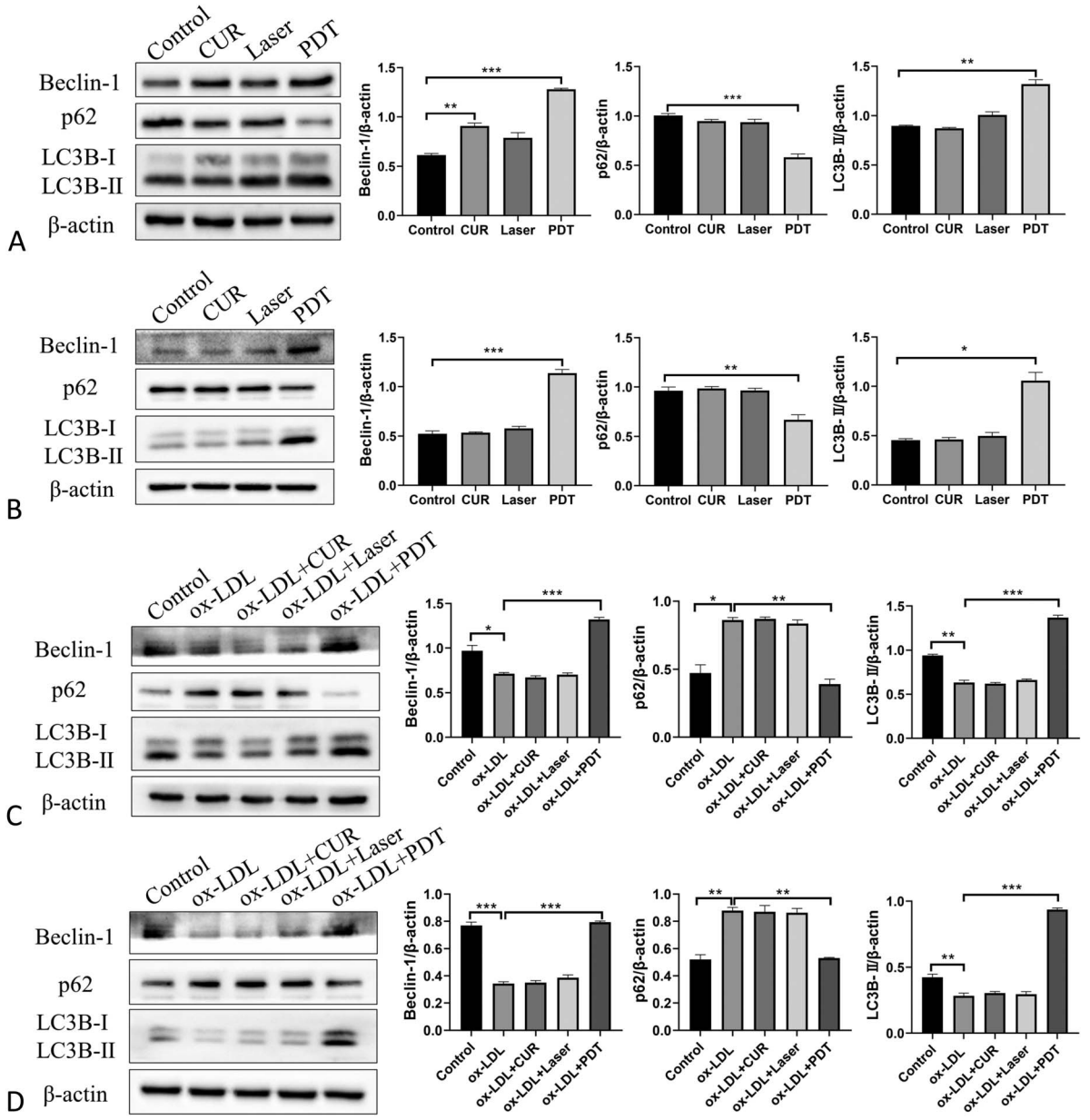

FIGURE 3. Effect of CUR-PDT on autophagy in VSMCs. The protein expression of Beclin-1, p62, and LC3B was detected by western blotting in VSMCs after different treatments for 6 hours. A, Effect of CUR-PDT on the expression of proteins related to autophagy in MOVAS cells; (B) effect of CUR-PDT on the expression of proteins related to autophagy in A7r5 cells; (C) effect of CUR-PDT on the expression of proteins related to autophagy in ox-LDL–treated MOVAS cells; and (D) effect of CUR-PDT on the expression of proteins related to autophagy in ox-LDL–treated A7r5 cells. n = 3 (3 independent experiments). Data are expressed as the mean ± SD. $*P < 0.05$, $**P < 0.01$, $***P < 0.001$.

first time that CUR-PDT inhibits phenotypic transformation, migration, and foaming of ox-LDL–treated VSMCs by promoting autophagy. This discovery overcomes the limitations of anti-AS treatment strategies and provides a new way of thinking and perspective for the treatment of AS.

It is well known that ox-LDL is closely related to the development of AS.[26–28] Therefore, we used the ox-LDL to induce the AS model. Two cells lines, MOVAS and A7r5 cell lines, were used to conduct parallel experiments simultaneously to ensure the reliability of our results. The 2 cell lines were used to select the optimal concentration of ox-LDL required to induce the AS model (see **Figure**, **Supplemental Digital Content 1**, http://links.lww.com/JCVP/A658). We first observed the effects of ox-LDL on VSMC-specific roles, and our results showed that under the induction of ox-LDL, the expression of the VSMC contraction phenotype proteins α-SMA and SM22-α was reduced, and the expression of the synthetic phenotype protein OPN

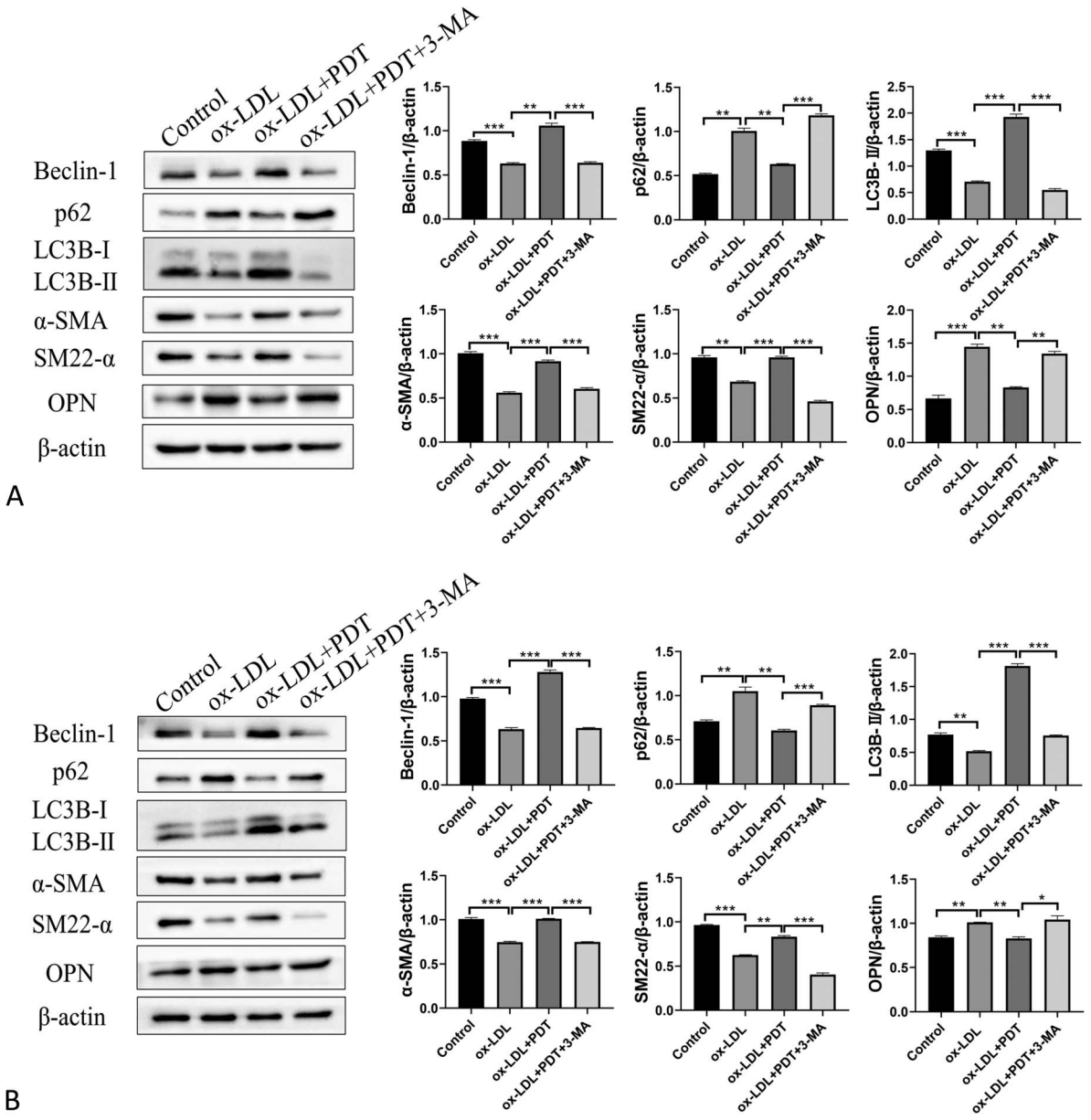

FIGURE 4. 3-MA reversed the effect of CUR-PDT on the phenotype transformation in VSMCs treated with ox-LDL. The expression of proteins related to autophagy (Beclin-1, p62, and LC3B) and proteins related to phenotype transformation (α-SMA, SM22-α, and OPN) were detected by western blotting in VSMCs after different treatments for 6 hours. A, Effect of 3-MA on the expression of proteins related to autophagy and proteins related to phenotype transformation in ox-LDL–treated MOVAS cells and (B) effect of 3-MA on the expression of proteins related to autophagy and proteins related to phenotype transformation in ox-LDL–treated A7r5 cells. n = 3 (3 independent experiments). Data are expressed as the mean ± SD. $*P < 0.05$, $**P < 0.01$, $***P < 0.001$.

was increased. At the same time, VSMC migration ability and the foaming degree were enhanced. These findings confirm that ox-LDL induces the transformation of VSMCs into a synthetic phenotype and promote their migration and foaming, which is consistent with previous reports.[28–30] In addition, we found that the expression of autophagy-related proteins Beclin-1 and LC3B-II and the degradation of p62 were suppressed by ox-LDL, suggesting that ox-LDL hindered VSMC autophagy. One study showed that activation of TRPV1 by capsaicin could rescue ox-LDL damaging autophagy in VSMCs.[23] Consistently, our results show that ox-LDL can retard autophagy in VSMCs.

Previous studies have shown that PDT mainly plays an antitumor role and inhibits AS plaque formation by inducing apoptosis.[31] However, PDT can also induce autophagy in cells through oxidative stress.[31–33] Studies related to AS have confirmed that PDT can promote the excretion of cholesterol by inducing autophagy in THP-1 macrophages and reduce the transformation of macrophages into foam cells.[24] In addition, as early as in the 1960s, Geer et al have first discovered

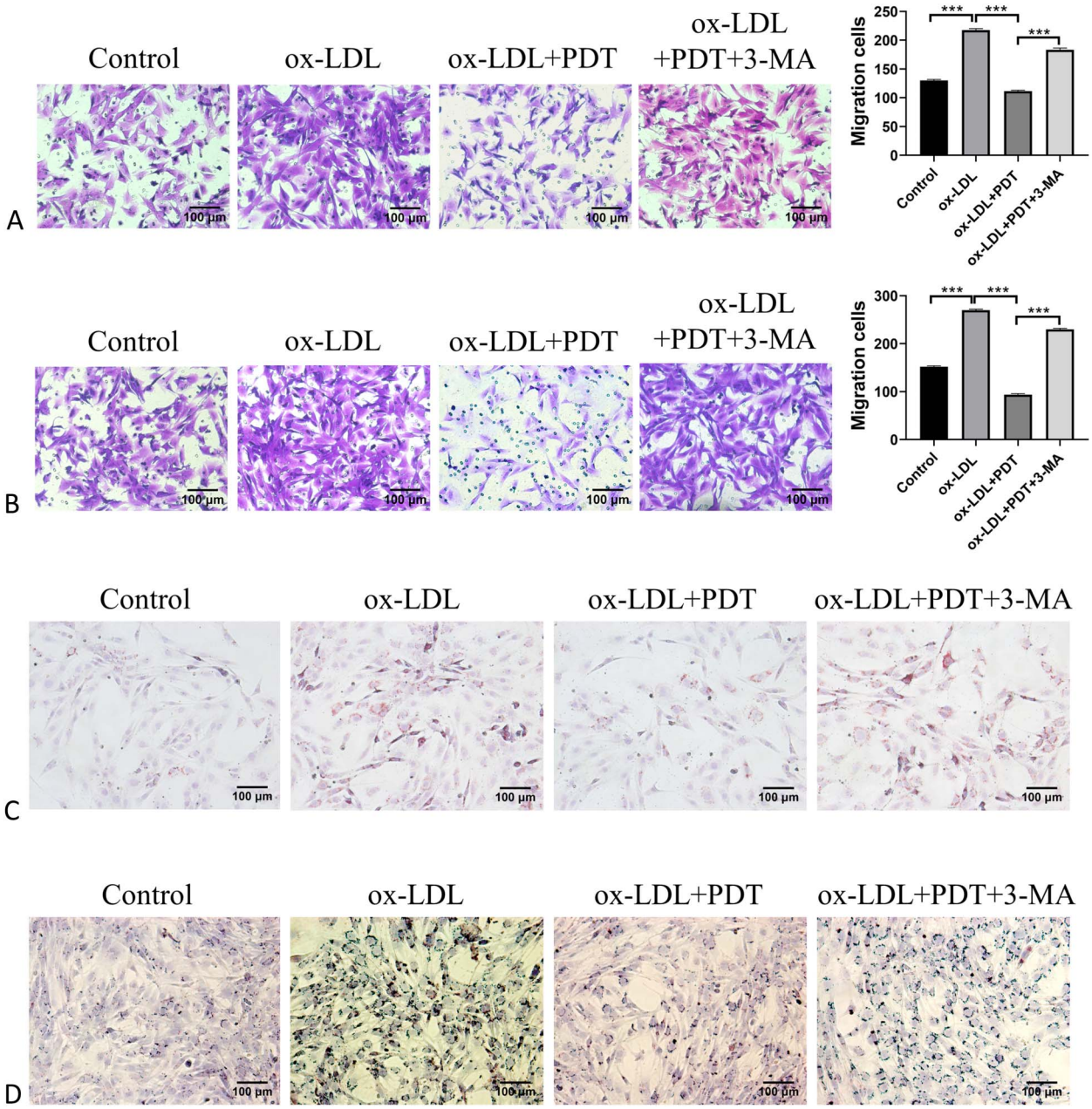

FIGURE 5. 3-MA reversed the effects of CUR-PDT on migration and lipid droplets accumulation in VSMCs treated with ox-LDL. Migration ability was detected by transwell assay. The accumulation degree of lipid droplets was measured by Oil Red O staining after CUR-PDT. A, Effect of 3-MA on migration ability in ox-LDL–treated MOVAS cells; (B) effect of 3-MA on migration ability in ox-LDL–treated A7r5 cells; (C) effect of 3-MA on accumulation of lipid droplets in ox-LDL–treated MOVAS cells; and (D) effect of 3-MA on accumulation of lipid droplets in ox-LDL–treated A7r5 cells. n = 3 (3 independent experiments). Data are expressed as the mean ± SD. $*P < 0.05$, $**P < 0.01$, $***P < 0.001$.

autophagy in plaques through transmission electron microscopy, and autophagy-related vesicle structures were mainly found in VSMCs.[34] Therefore, in this study, we combined CUR and PDT to intervene the ox-LDL–treated VSMCs. Our data showed that CUR-PDT increased the expression of the autophagy-related proteins Beclin-1 and LC3B-II and the degradation of p62, as well as increased the expression of the contraction phenotype of VSMC proteins α-SMA and SM22-α and decreased its synthetic phenotype protein expression of OPN. At the same time, VSMC migration was inhibited and lipid droplet accumulation was reduced in the PDT group. Based on the above data, we guess that CUR-PDT may inhibit phenotypic transformation and foaming of VSMCs by promoting autophagy. To further verify this result, we pretreated VSMCs with the autophagy inhibitor 3-MA before the CUR-PDT intervention, and the results

showed that all of the above results were reversed. These data confirmed that CUR-PDT inhibited the phenotype transformation and foaming by promoting autophagy in ox-LDL–treated VSMCs.

Although this study confirmed CUR-PDT about the regulation of autophagy and its specific role in inhibiting AS progression, it did not further explore the specific molecular mechanisms involved and lacked relevant experimental evidence in vivo. Autophagy is a complex metabolic process involving multiple links and multiple signals.[35] Rapamycin target protein (mTOR), as it is known, is a classic signaling pathway that regulates autophagy.[36] Previous studies have shown that ox-LDL can induce the formation of macrophage-derived foam cells by activating the mTOR signaling pathway, whereas blocking mTOR can inhibit the transformation, suggesting that the mTOR-autophagy pathway may also regulate its phenotype and function in VSMCs.[37] In addition, ucNPS-CE6-PDT has also been recently reported to inhibit the phosphorylation of Akt and mTOR in macrophage-derived foam cells.[38] Previous studies have found that CUR and its analogs can promote autophagy and intracellular lysosome regeneration by transcription factor EB in rat brain cells.[11,39] This suggests that CUR may promote autophagy through the mTOR-independent pathway, so whether CUR-PDT may also directly affect the expression and activation of transcription factor EB pathway–related molecules to participate in regulating VSMC autophagy, whose role and mechanism remain to be further explored. However, an increasing number of studies have focused on CUR resistance to AS in animals,[40–42] but the effects of CUR combined with PDT on AS in vivo have not been reported yet. Therefore, further validation of the above results in vivo remains to be performed in mice with autophagy gene knockout.

CONCLUSIONS

CUR-PDT inhibits the phenotypic transformation, migration, and foaming of ox-LDL–treated VSMCs by promoting autophagy. These findings are expected to provide a new theoretical basis for the treatment of AS.

ACKNOWLEDGMENTS

The Chongqing Key Laboratory of Translational Medicine in Major Metabolic Diseases, the First Affiliated Hospital of Chongqing Medical University, Chongqing, China.

REFERENCES

1. Libby P, Ridker P, Hansson G. Progress and challenges in translating the biology of atherosclerosis. *Nature*. 2011;473:317–325.
2. Bennett M, Sinha S, Owens G. Vascular smooth muscle cells in atherosclerosis. *Circ Res.* 2016;118:692–702.
3. Grootaert MO, Moulis M, Roth L, et al. Vascular smooth muscle cell death, autophagy and senescence in atherosclerosis. *Cardiovasc Res.* 2018;114:622–634.
4. Song W, Gao K, Huang P, et al. Bazedoxifene inhibits PDGF-BB induced VSMC phenotypic switch via regulating the autophagy level. *Life Sci.* 2020;259:118397.
5. Chistiakov D, Melnichenko A, Myasoedova V, et al. Mechanisms of foam cell formation in atherosclerosis. *J Mol Med (Berl).* 2017;95:1153–1165.
6. Allahverdian S, Chehroudi A, McManus B, et al. Contribution of intimal smooth muscle cells to cholesterol accumulation and macrophage-like cells in human atherosclerosis. *Circulation*. 2014;129:1551–1559.
7. Glukhova M, Ornatsky O, Frid M, et al. Identification of smooth muscle-derived foam cells in the atherosclerotic plaque of human aorta with monoclonal antibody IIG10. *Tissue Cell.* 1987;19:657–663.
8. Rosenfeld M, Ross R. Macrophage and smooth muscle cell proliferation in atherosclerotic lesions of WHHL and comparably hypercholesterolemic fat-fed rabbits. *Arteriosclerosis.* 1990;10:680–687.
9. Zhang HG, Kim H, Liu C, et al. Curcumin reverses breast tumor exosomes mediated immune suppression of NK cell tumor cytotoxicity. *Biochim Biophys Acta.* 2007;1773:1116–1123.
10. Huang H, Jan T, Yeh S. Inhibitory effect of curcumin, an anti-inflammatory agent, on vascular smooth muscle cell proliferation. *Eur J Pharmacol.* 1992;221:381–384.
11. Han J, Pan X, Xu Y, et al. Curcumin induces autophagy to protect vascular endothelial cell survival from oxidative stress damage. *Autophagy*. 2012;8:812–825.
12. Yuan HY, Kuang SY, Zheng X, et al. Curcumin inhibits cellular cholesterol accumulation by regulating SREBP-1/caveolin-1 signaling pathway in vascular smooth muscle cells. *Acta Pharmacol Sin.* 2008;29:555–563.
13. Gu H, Li H, Tang Y, et al. Nicotinate-curcumin impedes foam cell formation from THP-1 cells through restoring autophagy flux. *PLoS One*. 2016;11:e0154820.
14. Huang L, Chen Q, Yu L, et al. Pyropheophorbide-alpha methyl ester-mediated photodynamic therapy induces apoptosis and inhibits LPS-induced inflammation in RAW264.7 macrophages. *Photodiagnosis Photodyn Ther.* 2019;25:148–156.
15. Rkein A, Ozog D. Photodynamic therapy. *Dermatol Clin.* 2014;32:415–425, x.
16. Li K, Chen Q, Wang D, et al. Mitochondrial pathway and endoplasmic reticulum stress participate in the photosensitizing effectiveness of AE-PDT in MG63 cells. *Cancer Med.* 2016;5:3186–3193.
17. Jain M, Zellweger M, Wagnières G, et al. Photodynamic therapy for the treatment of atherosclerotic plaque: lost in translation? *Cardiovasc Ther.* 2017;35:2.
18. Yorimitsu T, Klionsky D. Autophagy: molecular machinery for self-eating. *Cell Death Differ.* 2005;12:1542–1552.
19. Hassanpour M, Rezabakhsh A, Pezeshkian M, et al. Distinct role of autophagy on angiogenesis: highlights on the effect of autophagy in endothelial lineage and progenitor cells. *Stem Cell Res Ther.* 2018;9:305.
20. Wu H, Song A, Hu W, et al. The anti-atherosclerotic effect of paeonol against vascular smooth muscle cell proliferation by up-regulation of autophagy via the AMPK/mTOR signaling pathway. *Front Pharmacol.* 2017;8:948.
21. Li J, Zhao L, Yang T, et al. c-Ski inhibits autophagy of vascular smooth muscle cells induced by oxLDL and PDGF. *PLoS One*. 2014;9:e98902.
22. Grootaert M, da Costa Martins P, Bitsch N, et al. Defective autophagy in vascular smooth muscle cells accelerates senescence and promotes neointima formation and atherogenesis. *Autophagy*. 2015;11:2014–2032.
23. Li BH, Yin YW, Liu Y, et al. TRPV1 activation impedes foam cell formation by inducing autophagy in oxLDL-treated vascular smooth muscle cells. *Cell Death Dis.* 2014;5:e1182.
24. Han XB, Li HX, Jiang YQ, et al. Upconversion nanoparticle-mediated photodynamic therapy induces autophagy and cholesterol efflux of macrophage-derived foam cells via ROS generation. *Cell Death Dis.* 2017;8:e2864.
25. Ray P, Huang B, Tsuji Y. Reactive oxygen species (ROS) homeostasis and redox regulation in cellular signaling. *Cell Signal.* 2012;24:981–990.
26. Koirala D, Beranova-Giorgianni S, Giorgianni F. Early transcriptomic response to OxLDL in human retinal pigment epithelial cells. *Int J Mol Sci.* 2020;21:8818.
27. Wu Y, Song F, Li Y, et al. Acacetin exerts antioxidant potential against atherosclerosis through Nrf2 pathway in apoE Mice. *J Cell Mol Med.* 2020;25:521–534.
28. Wang X, Li H, Zhang Y, et al. Suppression of miR-4463 promotes phenotypic switching in VSMCs treated with Ox-LDL. *Cell Tissue Res.* 2020;383:1155–1165.
29. Lu G, Chu Y, Tian P. Knockdown of H19 attenuates ox-LDL-induced vascular smooth muscle cell proliferation, migration and invasion by regulating miR-599/PAPPA axis. *J Cardiovasc Pharmacol.* 2020;77:386–396.

30. Pi H, Wang Z, Liu M, et al. SCD1 activation impedes foam cell formation by inducing lipophagy in oxLDL-treated human vascular smooth muscle cells. *J Cell Mol Med.* 2019;23:5259–5269.
31. Inguscio V, Panzarini E, Dini L. Autophagy contributes to the death/survival balance in cancer PhotoDynamic therapy. *Cells.* 2012;1:464–491.
32. Kessel D. Autophagic death probed by photodynamic therapy. *Autophagy.* 2015;11:1941–1943.
33. Waksman R, McEwan P, Moore T, et al. PhotoPoint photodynamic therapy promotes stabilization of atherosclerotic plaques and inhibits plaque progression. *J Am Coll Cardiol.* 2008;52:1024–1032.
34. Geer J, McGill H, Strong J. The fine structure of human atherosclerotic lesions. *Am J Pathol.* 1961;38:263–287.
35. Dong Y, Chen H, Gao J, et al. Molecular machinery and interplay of apoptosis and autophagy in coronary heart disease. *J Mol Cel Cardiol.* 2019;136:27–41.
36. Hou X, Hu Z, Xu H, et al. Advanced glycation endproducts trigger autophagy in cadiomyocyte via RAGE/PI3K/AKT/mTOR pathway. *Cardiovasc Diabetol.* 2014;13:78.
37. Wang X, Li L, Niu X, et al. mTOR enhances foam cell formation by suppressing the autophagy pathway. *DNA Cell Biol.* 2014;33:198–204.
38. Han X, Zhong Z, Kou J, et al. ROS generated by upconversion nanoparticle-mediated photodynamic therapy induces autophagy via PI3K/AKT/mTOR signaling pathway in M1 peritoneal macrophage. *Cell Physiol Biochem.* 2018;48:1616–1627.
39. Song J, Sun Y, Peluso I, et al. A novel curcumin analog binds to and activates TFEB in vitro and in vivo independent of MTOR inhibition. *Autophagy.* 2016;12:1372–1389.
40. Lv Y, Jia Y, Wan Z, et al. Curcumin inhibits the formation of atherosclerosis in ApoE mice by suppressing cytomegalovirus activity in endothelial cells. *Life Sci.* 2020;257:117658.
41. Gao S, Zhang W, Zhao Q, et al. Curcumin ameliorates atherosclerosis in apolipoprotein E deficient asthmatic mice by regulating the balance of Th2/Treg cells. *Phytomedicine.* 2019;52:129–135.
42. Meng N, Gong Y, Zhang J, et al. A novel curcumin-loaded nanoparticle restricts atherosclerosis development and promotes plaques stability in apolipoprotein E deficient mice. *J Biomater Appl.* 2019;33:946–954.